IJE Transactions C: Aspects Vol. 34, No. 9, (September 2021)

International Journal of Engineering

Journal Homepage: www.ije.ir

Effect of Additional Zirconia on Fracture Mechanics of Bioactive Glass-ceramics Using Digital Image Correlation

Israa K. Sabree, Mohsin A. Aswad, and Hadeer S. Abd Ali

Department of Ceramics Engineering and Building Materials, Faculty of Materials Engineering, University of Babylon, Babylon, P.O.Box:4, Iraq

P A P E R I N F O

Paper history:
Received 23 April 2021
Received in revised form 23 May 2021
Accepted 21 June 2021

Keywords:
Bioglass-ceramic
Zirconia nanoparticles
Composite material
Fracture toughness
Crack opening displacement
Digital image correlation

A B S T R A C T

Bioactive glass-ceramic is used as a replacement material for bone tissue due to its compatibility, bioactivity, and the ability to form a crystallized hydroxyapatite layer, which is similar in composition and structure to the inorganic component of the bone mineral phase. In this paper, bioglass-ceramic was toughened using zirconia to improve its mechanical behaviour (i.e. crack opening dsplacement and fracture toughness). The fracture toughness of the bioactive glass cerami/zirconia composite was measured using three-point bending technique. Digital Image Correlation (DIC) technique was utilized for visualized the crack initiation and calculation the crack opening displacement (COD) at the tip and mouth of the crack and measuring of the crack propagation of the bioactive glass cerami/zirconia composite. The results indicated that the incorporation of the zirconia particles improved the measured fracture toughness of the BGC/ZrO_2 composite. The toughness of composite bioceramics is enhanced due to crack branching and crack deflection due to the presence of zirconia particles.

doi: 10.5829/ije.2021.34.09c.01

NOMENCLATURE

COD	Crack Opening Displacement (mm)	**SEM**	Scanning Electron Microscope
BGC	Bioactive glass-ceramic	**K_{IC}**	Fracture Toughness (GPa.$m^{1/2}$)
XRD	X-ray Diffraction	**CMOD**	Crack Mouth Opening Displacement (mm)
ZrO_2	Zirconia	**CTOD**	Crack tip Opening Displacement (mm)

1. INTRODUCTION

Bioactive glass-ceramic is groups of osteoconductive biomaterial that assessed for restorating and repairing of body tissues especially for orthopedics and dental implant. According to the location and function of the damaged tissue, glass ceramics may require high strength and fracture toughness to be a suitable repairing material [1]. The central point limiting the use of bioactive ceramics is their low mechanical strength and fracture toughness. One approach to use ceramics as implants in load-bearing applications is reinforcing the ceramic with a second phase [2]. The mechanical properties of bioglass are controlled by the addition of oxides such as magnesia, alumina, zirconia, or titania. The use of composites of ZrO_2 and bioactive glass in the Na_2O–CaO–SiO_2–P_2O_5 system [3], where high strength comes from the zirconia reinforcing process and good compatibility and high bioactivity come from the bioactive glass, is an appealing way of producing strong bioactive materials [4]. Gali et al. [5] gave an evidence about increasing hardness and toughness of the glass ceramic-YSZ composites with varying amounts of YSZ (0, 5, 10, 15 and 20 wt.%). Kasuga et al. [1] confirmed the high bending strength of zirconia-toughened glass-ceramic composite with no degraded after in vivo implintation for 12 weeks, the optimum zirconia content to get high-strength and bioactivity was 30 vol.%. Rabiee and Azizian [6] used composite coating layer of bioactive glass–ceramic with various zirconia concentrations; the hardness test demonstrate that increasing zirconia content lead to rising of coating hardness. Zirconia was used to resolve the issue of ceramic brittleness and the resultant potential failed implants [7]. Fracture mechanics is a subject of engineering science that deals with the failure of solids caused by crack initiation and propagation [8], cracks are everywhere around us, these cracks which often exist could result in from industrial flaws or a variety of environmental conditions in the course of loading. Crack opening displacement and crack propagation are the most important parameters in fracture mechanics [9]. Fracture mechanics is depended on the stress intensity factor, wich

is describes the stress concentration at the crack tip [10]. Measuring the crack opening displacement is difficult and as values obtain smaller, distinct equipment is needed and for a ceramic, SEM has been utilized [11]. These methods require precise sample preparations and distinctive care for determining the precise value of displacements [12-13]. To solve these challenges, non-contact optical technologies such as (DIC) Digital Image Correlation, which are used to determine the displacements and strains of samples for detecting crack propagation and measuring crack opening displacement, can be used to acquire a procedure for measuring the displacement of a specific location and precise strain measurements [14-15]. The aim of the study to improve the mechanical behaviour (i.e crack opening displacement and frcature toughness) of the bioactive glass ceamic tougheneing using zirconia and using digital image correlation for visualization of the crack initiation and measuring crack opening displacement and propagation in BGC/ ZrO_2 composite.

2. EXPERIMENTAL PROCEDURES

2.1 Materials Preparation

Bioglass-ceramic was prepared by melting technique. The preparation method and characterization were explained by Aswad et al. [16] and zirconia-yttria nanopowder/ nanoparticles (ZrO_2-3Y, 99.95%, 20 nm, metal basis).

2.2 Bioglass-Ceramic / Zirconia Composite

The composites were prepared from mixing different amounts of zirconia-yttria nanopowder/ nanoparticles (ZrO_2-3Y, 99.95%, 20 nm, metal basis) with prepared bioglass-ceramic powders. Where was mixed (3,5) wt.% of ZrO_2 nanopowder with bioglass-ceramic powder by using magnetic stirrer for 6 h using ethanol as solvent. The resulting slurry dried at 120 ^oC in the oven for 48 h. The dried powder was then crushed and sieved to be ready for compaction.

2.3 Compact of BGC ansd BGC/ZrO_2 Specimens

Bioglass-ceramic and BGC/ ZrO_2 powders were mixed with (2 wt %) poly vinyl alcohol, PVA as a binder's material [17]. Uniaxial semi-dry pressing techniques were used to form green ceramics specimens utilizing rectangles molds made of stainless steel with (60×6×5 mm) dimension. Figure 1 shows the compacts specimen for the fracture test. The appropriate pressure was 150 MPa. Solid specimens were bonded by sintering at temperatures 1000 °C with the heating rate (10°C/min) and soaking time 3 h and cooling down inside the furnace.

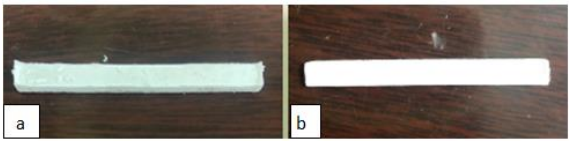

Figure 1. show compacts specimens for fracture test (a) before sintering, (b) after sintering with surface finishing (grinding and polishing).

2.4 Single Edge Notched Beam Sample

Figure 2 shows the sample with dimensions (3 ×4 ×50) mm, and the samples were prepared to study fracture using a single edge notch beam [18]. Notch was made using a 170 μm thick diamond cutting disk (BT-MS210) in the ceramic laboratory/ Material Engineering College/ Babylon University [19].

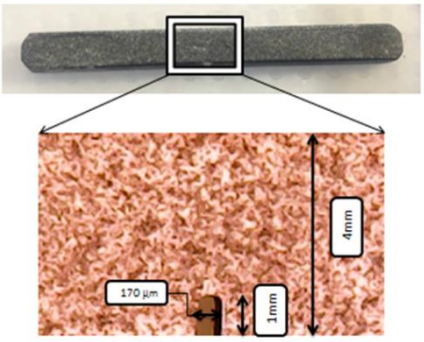

Figure 2. BGC/ ZrO_2 composite specimen after created Notched using SENB method.

2.5 Digital Image Correlation

The DIC method is an optical technique, which utilizes the full field, non-contact and high precision measurement of deformations and displacements. The artificial speckles pattern was created by sprayed randomly with black paint (vinyl acetate/ethylene VAE) on the BGC/ ZrO_2 composite specimen surface as shown in Figure 3. The speckles pattern are required to be non-repetitive, isotropic and contrast enough to permit the software to be able to identify and match the image before and after deformation [20-21]. The sprayed of a sample is necessary to make a subset, as shown in Figure 4. The software of DIC used for calculation named GOM (Gesellschaft fur Optische Mebtechnik) from a German company. These calculations start with a reference image captured before loading that was compared with other images during the loading periods. The assumption proposed was that the color values of the image remain the same before and after the deformations. Firstly, the images are divided into subsets and look for the corresponding subset after deformations based on the assumptions and calculate their displacement; finally, deformations or displacement distributions maps are

made. Figure 5 shows using digital image correlation for displacement measurement.

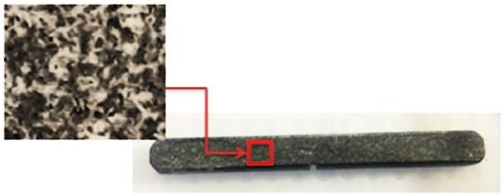

Figure 3. Speckles of black paint

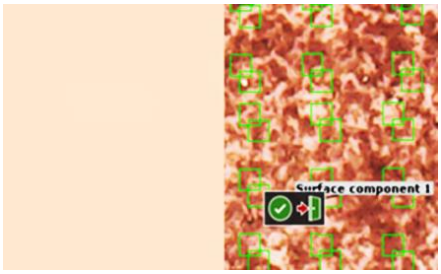

Figure 4. Subsets show when speckles of black paint (right side), unlike without black paint (left side)

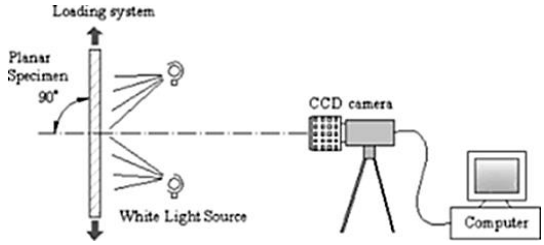

Figure 5. Setup for displacement measurement using digital image correlation [20]

2.6 Loading Setup and Test Procedure

Specimens were subjected to the load microcomputers controlled electronics universal testing machines. These testing machines have loadings capacities of 5 KN and the loading rates are very low, resulting in a displacement not exceeding 0.005 mm/min. This camera is a digital microscope camera (Genesys Logic), and it has a lamp that is used to lighten the speckle pattern and is adapted to capture digital images during the loading process. The camera was positioned such that its lens was as parallel to the specimen surface as possible, and the focal length was changed to ensure that the picture was clear. The resolution of the camera was set to 640 × 480 pixels and the length pixel ratios of the imaging systems are 0.0008 mm/pixel. Cameras were programmed for capturing the image automatically at frames rates of 30 images/s, and these frames rates suit to store and to capture large numbers of images for further. The DIC method is to match maximum correlation between small zones (or subsets) of the specimen according to equations below:

$$R(x, y, x^*, y^*) = \sum F(x, y) - G(x^*, y^*) \quad (1)$$

$$C(x, y, x*, y*) = \frac{\sum F(x,y)\, G(x*,y*)}{\sqrt{\sum F(x,y)^2 \sum G(x*,y*)^2}} \quad (2)$$

2.7 Measurement of The Crack Opening Displacement

The position of crack mouth and crack tip opening displacement can be noticed in Figure 6 [22]. The crack opening displacement (CMOD and CTOD) can be measured throw DIC using two curves as shown in Figure 7. By the crack opening calculation with distance checks, you can analyze how the distance between two curves deviates from a reference value. The reference value can be a nominal value or a distance in the first active stage.

Figure 6. Position of CMOD and CTOD in GOM

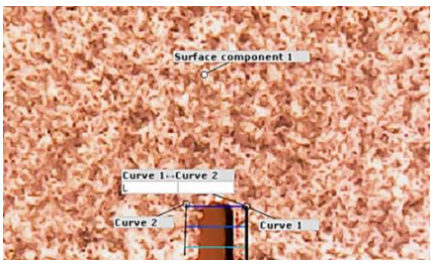

Figure 7. Measurement of CMOD and CTOD

3. RESULTS AND DISCUSSION

3.1 Fracture Toughness

The fracture toughness of samples is known to be affected by the crack propagation behavior of composites [23]; thus, crack deflection and crack branching increase fracture toughness in the presence of ZrO_2 particles in the matrix. As the crack front interacts with a second-phase inclusion, such as ZrO_2 particles, the crack propagates out of the plane, lowering the stress intensity factor at the crack tip. To put it another way, it slows down crack propagation because it takes more energy to propagate a crack [24-25]. Crack deflection may be caused by residual stress in the composite or weak matrix/second phase interfaces [26].

The fracture toughness of this study was calculated according to ASTM C1421 as shown below:

$$K_{Ic} = g\left[\frac{P_{max}\, S_o\, 10^{-6}}{BW^{3/2}}\right]\left[\frac{3[a/W]^{1/2}}{2[1-a/W]^{3/2}}\right] \quad (3)$$

TABLE 1. Fracture toughness of BGC and composites

sample	Fracture Toughness ($MPa.m^{1/2}$)
Pure BGC	0.75
BGC / 3%ZrO_2	1.04
BGC / 5%ZrO_2	1.61

3.2 Toughening Mechanism

The toughening mechanisms were investigated by Vickers' indentations were made on the polished surfaces and the cracks propagations path was as shown in Figure 8. The cracks of the BGC specimen show a transgranular fracture behavior, indicating that the toughness of BGC is independent of its grain size. Because of this transgranular fracture behavior, very straight cracks are often observed radiating from indentation corners, as shown in Figure 9, for the sample with 5wt.% ZrO_2. The crack is deflected when it encounters zirconia particles. Sometimes crack branching occurs by zirconia particles. Therefore, the toughening is attributed to both crack deflection and crack branching at sites of zirconia particles[25-27].

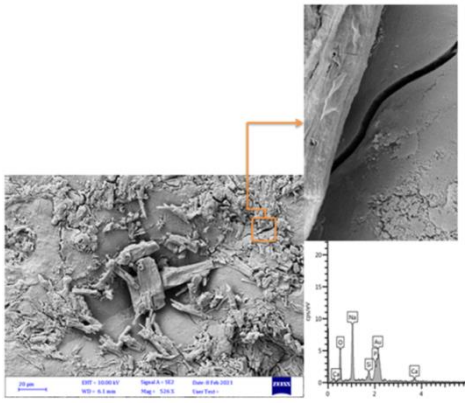

Figure 8. Indentation crack propagation pattern in pure bioglass-ceramic sample sintered at 1000°C

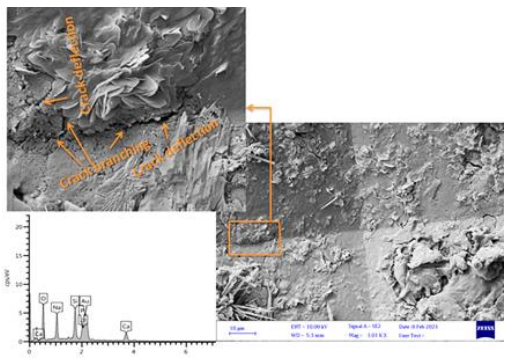

Figure 9. Indentation crack propagation pattern in BGC/5wt.% ZrO_2 sample sintered at 1000°C

3.3 Visualization and Propagation of Cracks

DIC is a good method for visualized the crack and its initiation, otherwise, these cracks are not visible without using the DIC technique [28]. The results obtained from DIC to identified crack propagation with load and time of pure BGC and BGC-3, 5wt.% ZrO_2 is shown in Figure 10, respectively. These figures show the change in strain mapping near the notch at different loads and times for bioglass-ceramic and composite samples. Each figure contains six images, The image (a) in every figure shows the undeformed sample (before applied loading), image (b) doesn't show a change in strain mapping near the notch tip, whereas the image (c) shows change in strain mapping near the notch tip which indicates to stress concentration near the notch tip. Critical load and crack have been formed as shown in image (d). Thereafter the specimen losing the bearing capacity and load rapidly decrease when the crack propagated as shown in images (e) and (f).The critical load for pure BGC (11 N) and the time when crack initiation was 412s. Also from this figure can be noticed that the critical load for (BGC-3wt.% ZrO_2) is 15 N at critical time 712s while the critical load for (BGC-5wt.% ZrO_2) is 22 N at critical time 1637s. The effect of addition ZrO_2 to bioglass-ceramic enhanced fracture toughness of bioglass-ceramic.

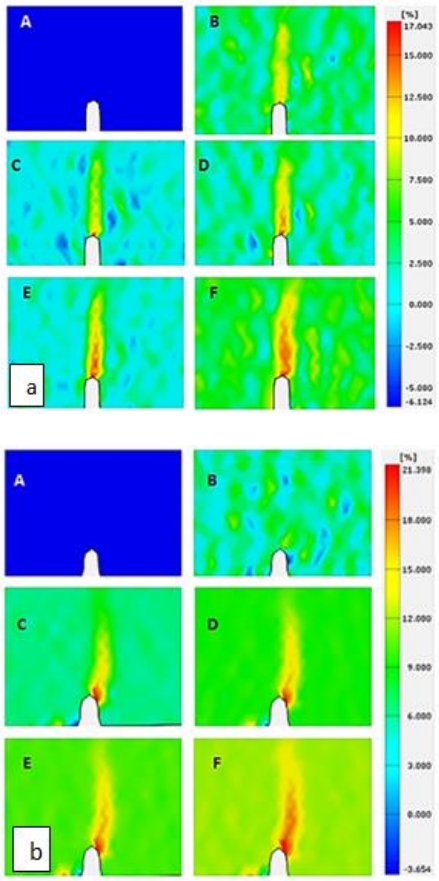

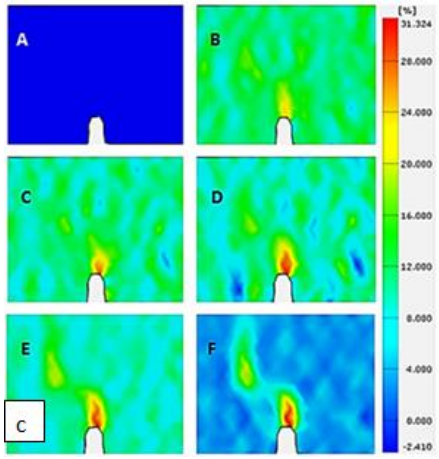

Figure 10. Strain maps with different load and time (a) Pure BGC,(b) BGC-3wt.% ZrO_2, (c) BGC-3wt.% ZrO_2

Figure 11 shows the relationship between load and time, in the SENB method. The curved divides into three parts: The first part represents the lower slope, it is before and the beginning of the emergence of the crack, The second part is steeper slope represents crack propagation before reaching the critical load, the top peak is represented a critical load. The last part is after the arrival of the sample to the critical load and continues to progress rapidly until the specimen fails.

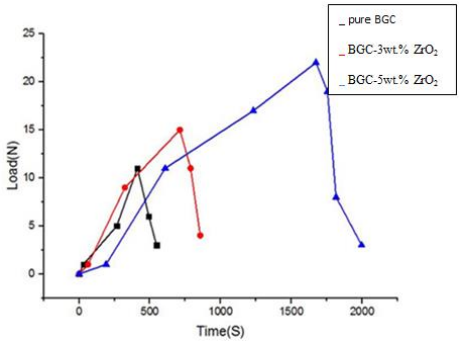

Figure 11. Represent the relationship between the load versus time of all specimens

3.4 Crack Opening Displacement of Specimen

The relationship between applied force and crack opening displacement (CMOD and CTOD) [29] shown in Figure 12. From this figure can notice the force versus COD curve can be divided into three parts. In the first part, the relationship is linear, the second part start as soon as the curve deviates from linearity. The crack opening begins to widen at a faster rate, signaling the onset of material damage. The load continues to rise in this section until the peak load value is reached, at which point the material's full loading capacity is reached. As the crack mouth opening displacement continues to increase and the load begins to decrease after the peak load level, the last part begins [30].

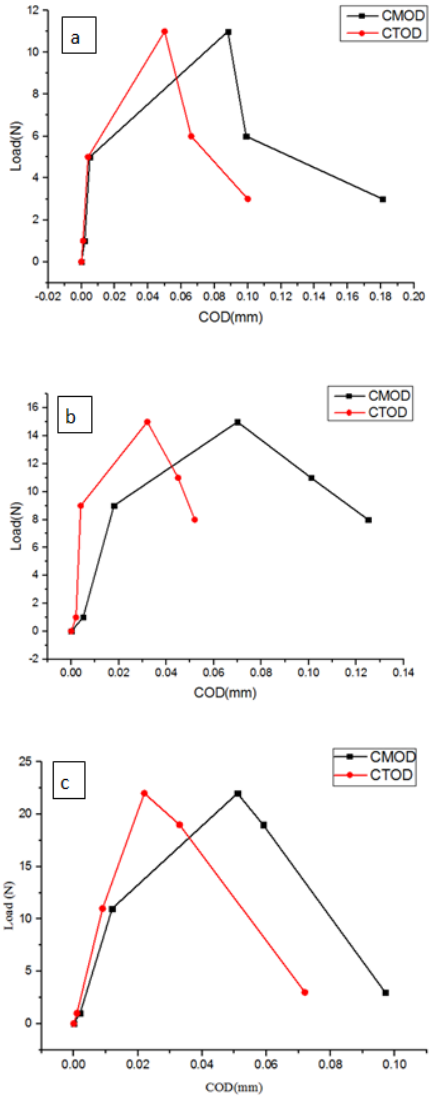

Figure 12. Load versus COD (a) BGC pure, (b) BGC-3wt.% ZrO_2, (c) BGC-5wt.% ZrO_2

4. CONCLUSIONS

According to the results of the experimental work, can be concluded the DIC is a good method for visualizetion of the crack initiation and measuring crack opening and propagation in BGC/ ZrO_2 composite. The critical stress intensity factor (K_{IC}) of BGC, BGC with 3, and 5wt.% ZrO_2 was 0.75, 1.04, and 1.61 MPa. $\sqrt{m}$ respectively, and the critical load of BGC, BGC/3, and 5 wt.% ZrO_2 were 11, 15, and 22 N, respectively for the experimental result.

5. REFERENCES

[1] Kasuga. T., Yoshida. M., Ikushima A. J., M. Tuchiya, and Kusakar H.i, "Stability of zirconia-toughened bioactive glass-ceramics: in vivo study using dogs," ***Journal of Materials Science: Materials in Medicine***, vol. 4, no. 1, pp. 36–39, 1993. https://doi.org/10.1007/BF00122975.

[2] Hench L. L., *An introduction to bioceramics*, vol. 1. World scientific, 1993. https://doi.org/10.1142

[3] Trang G. T., Linh N. H., and Kien P. H., "The study of dynamics heterogeneity in SiO2 liquid," ***HighTech Innovation Journal,*** vol. 1, no. 1, pp. 1–7, 2020. DOI: 10.28991/HIJ-2020-01-01-01

[4] Elgayar I., Aliev A. E., Boccaccini A. R., and Hill R. G., "Structural analysis of bioactive glasses," ***Journal of Non-Crystalline Solids***, vol. 351, no. 2, pp. 173–183, 2005. https://doi.org/10.1016/j.jnoncrysol.2004.07.067

[5] Gali S., Ravikumar K., Murthy B. V. S., and Basu B., "Zirconia toughened mica glass ceramics for dental restorations," ***Dental Materials***, vol. 34, no. 3, pp. e36–e45, 2018. doi: 10.1016/j.dental.2018.01.009.

[6] Rabiee S. M. and Azizian M., "Effect of zirconia concentration on the growth of nanowires in bioactive glass–ceramic coatings," ***International Journal of Applied Ceramic Technology,*** vol. 10, no. 1, pp. 33–39, 2013. https://doi.org/10.1111/j.1744-7402.2012.02844.x

[7] Christel P. *et al.*, "Biomechanical compatibility and design of ceramic implants for orthopedic surgery," ***Annals of the New York Academy of Sciences***, vol. 523, no. 1, pp. 234–256, 1988. doi: 10.1111/j.1749-6632.1988.tb38516.x

[8] Sun C. T. and Jin Z. H., "Fracture Mechanics," pp. 7–8, 2012, doi: 10.1016/B978-0-12-385001-0.00001-8.

[9] Nunes L. C. S. and Reis J. M. L., "Estimation of crack-tip-opening displacement and crack extension of glass fiber reinforced polymer mortars using digital image correlation method," ***Materials & Design***, vol. 33, pp. 248–253, 2012. https://doi.org/10.1016/j.matdes.2011.07.051

[10] Dalmas D., Barthel E., and Vandembroucq D., "Crack front pinning by design in planar heterogeneous interfaces," ***Journal of the Mechanics and Physics of Solids***, vol. 57, no. 3, pp. 446–457, 2009, doi: 10.1016/j.jmps.2008.11.012.

[11] Nguyen P. D., Dang V. H., and Eduardovich P. A., "Long-term Deflections of Hybrid GFRP/Steel Reinforced Concrete Beams under Sustained Loads," ***Civil Engineering Journal,*** vol. 6, pp. 1–11, 2020. DOI: 10.28991/cej-2020-sp(emce)-01

[12] Lin Z. X., Xu Z. H., An Y. H., and Li X., "In situ observation of fracture behavior of canine cortical bone under bending," ***Materials Science and Engineering: C,*** vol. 62, pp. 361–367, 2016, doi: 10.1016/j.msec.2016.01.061.

[13] Mekky W. and Nicholson P. S., "The fracture toughness of Ni/Al2O3 laminates by digital image correlation I: experimental crack opening displacement and R-curves," ***Engineering Fracture Mechanics,*** vol. 73, no. 5, pp. 571–582, 2006.

[14] Brynk T., Laptiev A., Tolochyn O., and Pakiela Z., "Digital Image Correlation Based Method of Crack Growth Rate and Fracture Toughness Measurements on Mini-Samples," ***Key Engineering Materials,*** vol. 586, pp. 96–99, 2014, doi: 10.4028/www.scientific.net/KEM.586.96.

[15] Lyubutin P. S. and Panin S. V., "Mesoscale measurement of strains by analyzing optical images of the surface of loaded solids," ***Journal of applied mechanics and technical physics***, vol. 47, no. 6, pp. 905–910, 2006. https://doi.org/10.1007/s10808-006-0131-z

[16] Aswad M. A., Sabree I. K., and Abd Ali H S, "An examination of the effect of adding zirconia to bioactive glass-ceramic properties," *IOP* ***Conference. Series Material Science Engineering***, vol. 1067, no. 1, p. 012121, 2021, doi: 10.1088/1757-899x/1067/1/012121.

[17] Gharibshahian E., "The Effect of Polyvinyl Alcohol Concentration on the Growth Kinetics of KTiOPO4 Nanoparticles Synthesized by the Co-precipitation Method," ***HighTech Innovation Journal***, vol. 1, no. 4, pp. 187–193, 2020. Doi: 10.28991/HIJ-2020-01-04-06

[18] Singh A., Kumar S., and Yadav H. L., "Experimental and Numerical Investigation of Fracture Parameters for Side Edge Notch Bend Specimen of Al 6063-T6," ***Iranian Journal of Science and Technology, Transactions of Mechanical Engineering,*** pp. 1–19, 2020. https://doi.org/10.1007/s40997-020-00352-x

[19] McCormack X., Wang J., Stover S. G. J., and Fyhrie D. "Effects of Mineral Content on the Fracture Properties of Equine Cortical Bone in Double Notched Beams," ***Bone,*** Vol. *50 No.* 6 (2012), 1275-1280., doi: 10.1016/j.bone.2012.02.018

[20] Pan B., Qian K., Xie H., and Asundi A., "Two-dimensional digital image correlation for in-plane displacement and strain measurement: a review," ***Measurement Science and Technology***, vol. 20, no. 6, p. 062001, 2009, doi: 10.1088/0957-0233/20/6/062001.

[21] Albo-Jasim M. M. H., Aswad M A., and Rashed H K., "Investigation of Crack Propagation and Opening in Hydroxyapatite Using Digital Image Correlation."***Journal of Engineering and Applied Sciences***, 12, 7953-7943, 2017. DOI: 10.3923/jeasci.2017.7935.7943 .

[22] Panin S. V., Titkov V. V, and Lyubutin P. S., "Incremental approach to determination of image fragment displacements during vector field construction," ***Optoelectronics, Instrumentation and Data Processing,*** vol. 50, no. 2, pp. 139–147, 2014. https://doi.org/10.3103/S8756699014020058

[23] Panin S. V., Maruschak P. O., Lyubutin P. S., Konovalenko I. V, and Ovechkin B. B., "Application of meso-and fracture mechanics to material affected by a network of thermal fatigue cracks," ***International Journal of Fatigue***, vol. 76, pp. 33–38, 2015. https://doi.org/10.1016/j.ijfatigue.2014.10.013

[24] Faber K. T. and Evans A. G., "Crack deflection processes—I. Theory," ***Acta Metallurgica***, vol. 31, no. 4, pp. 565–576, 1983. https://doi.org/10.1016/0001-6160(83)90046-9

[25] Rejab N. A., A. Azhar Z. A., Ratnam M. M., and Ahmad Z. A., "The relationship between microstructure and fracture toughness of zirconia toughened alumina (ZTA) added with MgO and CeO2," ***International Journal of Refractory Metals and Hard Materials***, vol. 41, pp. 522–530, 2013. https://doi.org/10.1016/j.ijrmhm.2013.07.002

[26] Bengisu M. and Inal O. T., "Whisker toughening of ceramics: toughening mechanisms, fabrication, and composite properties," ***Annual Review of Materials Science,*** vol. 24, no. 1, pp. 83–124, 1994. https://www.annualreviews.org › doi

[27] Abbas S., Maleksaeedi S., Kolos E., and Ruys A. J., "Processing and properties of zirconia-toughened alumina prepared by gelcasting," ***Materials*** *(Basel).*, vol. 8, no. 7, pp. 4344–4362, 2015. doi: 10.3390/ma8074344

[28] Panin S. V, Chemezov V. O., Lyubutin P. S., and Titkov V. V, "Algorithm of fatigue crack detection and determination of its tip position in optical images," ***Optoelectronics, Instrumentation and Data Processing***, vol. 53, no. 3, pp. 237–244, 2017. https://doi.org/10.3103/S8756699017030062

[29] Kaaim A. H.. Aswad M A., Awad S H, "Study on Iraqi bauxite ceramic reinforced Aluminum metal matrix composite synthesized by stir casting." ***International Journal of Engineering, Transactions A: Basics,*** Vol. 33, no. 7 (2020): 1331-1339. 10.5829/IJE.2020.33.07A.20

[30] Marques B., Neto D., Antunes F., Vasco-Olmo J., and Díaz F., "Numerical tool for the analysis of CTOD curves obtained by DIC or FEM," ***Fatigue & Fracture of Engineering Materials & Structures,*** vol. 43, no. 12, pp. 2984–2997, 2020. https://doi.org/10.1111/ffe.13350

سرامیک شیشه ای زیست فعال به دلیل سازگاری ، فعالیت زیستی و توانایی تشکیل یک لایه هیدروکسی آپاتیت متبلور ، که از نظر ترکیب و ساختار مشابه با اجزای غیر آلی فاز مواد معدنی استخوان است ، به عنوان ماده جایگزینی برای بافت استخوان استفاده می شود. در این مقاله ، سرامیک بیوگلاس با استفاده از زیرکونیا برای بهبود رفتار مکانیکی آن (به عنوان مثال محل انعطاف پذیری بازشو و مقاومت در برابر شکست) سخت شد. مقاومت در برابر شکست کامپوزیت شیشه زیستی فعال / سرامیک با استفاده از روش خمش سه نقطه ای اندازه گیری شد. از روش همبستگی تصویر دیجیتال DIC برای تجسم شروع ترک و محاسبه جابجایی بازشدگی ترک (COD)در نوک و دهان ترک و اندازه گیری انتشار ترک ترکیبی از سرامیک شیشه ای / زیرکونیا استفاده شده است. نتایج نشان داد که ترکیب ذرات زیرکونیا مقاومت شکستگی اندازه گیری شده کامپوزیت BGC / ZrO_2 را بهبود می بخشد. مقاومت بیوسرامیک کامپوزیت به دلیل انشعاب ترک و انحراف ترک به دلیل وجود ذرات زیرکونیا افزایش می یابد.